IX CONGRESSO BRASILEIRO DE ENGENHARIA E CIÊNCIAS TÉRMICAS
9th BRAZILIAN CONGRESS OF THERMAL ENGINEERING AND SCIENCES

Paper CIT02-0903

NUMERICAL SIMULATION OF THE FLOW AROUND A SQUARE CYLINDER USING THE VORTEX METHOD

Vanessa Gonçalves Guedes
Department of Mechanical Engineering, EE/COPPE/UFRJ
C.P. 68503 CEP : 21945-970 Rio de Janeiro, RJ, Brazil
vanessag@cepel.br

Gustavo César Rachid Bodstein
Department of Mechanical Engineering, EE/COPPE/UFRJ
C.P. 68503 - CEP : 21945-970 Rio de Janeiro, RJ, Brazil
Tel: (021) 562-8406; fax: (021) 290-6626
gustavo@serv.com.ufrj.br

Miguel Hiroo Hirata
Department of Mechanics, Mechanical Engineering Institute, EFEI
C.P. 50 - CEP : 37500-000 Itajubá, MG, Brazil
hirata@iem.efei.br

Abstract. *The study of external incompressible flows at high Reynolds numbers around bluff bodies finds extensive applicability to real-life problems, in addition to the recently renewed scientific interest as a means for testing numerical algorithms. Such flows are characterized by several different regimes that depend on the value of the Reynolds number, ranging from steady Stokes-type flows to strongly unsteady turbulent flows. For a wide range of Reynolds numbers a Von Karman-type periodic wake is formed. In most cases the occurrence of separation makes the prediction of these flows very difficult, and one has to rely on specific experimental data to calculate the aerodynamic forces on the body. Many attempts to numerically simulate most of the flow details have been reported in the literature, and a variety of both mesh-based and mesh-free methods have been used.*
*In this paper we use a new mesh-free two-dimensional discrete vortex method associated to a method of distributed singularities, the Panel Method, to calculate global (*e.g. *lift and drag coefficients) as well as local (*e.g. *pressure coefficient) quantities for a high Reynolds number flow around a square cylinder. Lamb vortices are generated along the cylinder surface, whose strengths are determined to ensure that the no-slip condition is satisfied and that circulation is conserved. The impermeability condition is imposed through the application of a source panel method, so that mass conservation is explicitly enforced. The dynamics of the body wake is computed using the convection-diffusion splitting algorithm, where the diffusion process is simulated using the random walk method, and the convection process is carried out with a lagrangian second-order time-marching scheme. Results for the aerodynamic forces and pressure distribution are presented.*

Keywords. *Fluid Mechanics, Aerodynamics, Bluff Bodies, Incompressible Flows, Gas Dynamics.*

1. Introduction

In this work, we use the Vortex Method associated to the Panel Method, which models the flow past an square cylinder as the summation of a uniform flow (same speed and direction everywhere) and a series of panels arranged to form a closed polygon with a shape that approximates, as nearly as possible, the actual shape of the bluff body. Panel methods are techniques for solving potential flow over 2-D and 3-D geometries. The governing equation (Laplace's equation, or the linearized form in compressible flow) is recast into an integral equation. This integral equation involves quantities such as velocity, only on the surface, whereas the original equation involved the velocity potential all over the flow field. The surface is divided into panels or "boundary elements", and the integral is approximated by an algebraic expression on each of these panels. A system of linear algebraic equations result for the unknowns at the solid surface, which may be solved using techniques such as Gaussian elimination to determine the unknowns at the body surface.

With this new mesh-free method, we calculate global (*e.g.* lift and drag coefficients) as well as local (*e.g.* pressure coefficient) quantities for a high Reynolds number flow around a square cylinder. Lamb vortices are generated along the cylinder surface, whose strengths are determined to ensure that the no-slip condition is satisfied and that circulation is conserved. The impermeability condition is imposed through the application of a source panel method, so that mass conservation is explicitly enforced. The dynamics of the body wake is computed using the convection-diffusion splitting algorithm, where the diffusion process is simulated using the random walk method, and the convection process is carried out with a lagrangian second-order time-marching scheme. Results for the aerodynamic forces and pressure distribution are presented.

2. Mathematical Formulation

We begin our analysis considering the flow around a circular cylinder of radius a, immersed in an unbounded region with a uniform flow and freestream speed U (Fig. 1). We assume the flow to be incompressible and two-dimensional, and the fluid to be newtonian with constant kinematic viscosity ν. The unsteady flow that develops originates from the separation that occurs on the cylinder surface, which generates an oscillatory wake downstream of the body. This flow is governed by the continuity and the Navier-Stokes equations, which can be written in the form

$$\nabla \cdot \mathbf{u} = 0\,, \tag{1}$$

$$\frac{\partial \mathbf{u}}{\partial t} + \mathbf{u} \cdot \nabla \mathbf{u} = -\nabla p + \frac{1}{Re}\nabla^2 \mathbf{u}\,. \tag{2}$$

In the equations above **u** is the velocity vector field, p is the pressure, and $Re \equiv aU/\nu$ is the Reynolds number based on the square cylinder length side a. All the quantities in Eqs. (1), (2) and the equations below are nondimensionalized by U and a.

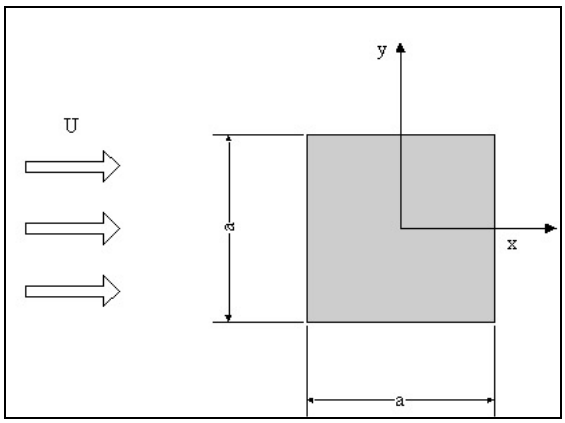

Figure 1. Flow around a square cylinder.

For all the cases studied, the flow is started impulsively from rest. The impermeability and the no-slip boundary conditions on the surface of the cylinder can be expressed as

$$u_n \equiv \mathbf{u} \cdot \mathbf{n} = 0\,, \text{ at } r = 1\,, \tag{3}$$

$$u_t \equiv \mathbf{u} \cdot \mathbf{t} = 0\,, \text{ at } r = 1\,, \tag{4}$$

where **n** and **t** are unit vectors normal and tangential to the cylinder surface, respectively. At infinity we require that

$$|\mathbf{u}| \to 1\,, \text{ as } r \to \infty\,. \tag{5}$$

The dynamics of the fluid motion, governed by the boundary-value problem (1)-(5), can be studied in a more convenient way if we take the curl of Eq. (2) to obtain the vorticity equation. For a 2-D flow this equation is scalar, and it can be written as

$$\frac{\partial \omega}{\partial t} + \mathbf{u} \cdot \nabla \omega = \frac{1}{Re}\nabla^2 \omega\,, \tag{6}$$

where ω is the only non-zero component of the vorticity vector (in a direction normal to the plane of the flow).

In our model, the vorticity in the flow is represented by a cloud of discrete point vortices. Using the source panel method, (Anderson Jr., 1985), we can combine this point-vortex representation with a uniform flow and constant source strength (λ_j) distribution to construct a flow field (see Fig.2) such that Eqs. (1), (3) and (5) are automatically satisfied. Thus, two mathematical expressions for the velocities components are given by Eqs. (7) and (8) and the variables involved are shown in Fig.3.

$$u(x,y) = 1 + \sum_{j=1}^{np} \frac{\lambda_j}{2\pi}\left(\frac{C_u}{2} \ln\left(\frac{Sp_j^2 + 2ASp_j + B}{B} \right) + \frac{D_u - AC_u}{E}\left(\tan^{-1}\frac{Sp_j + A}{E} - \tan^{-1}\frac{A}{E} \right) \right) - \frac{1}{2\pi}\sum_{j=1}^{N_v} \Gamma_k \frac{(y - y_j)}{(x - x_j)^2 + (y - y_j)^2} \tag{7}$$

and

$$v(x,y) = \sum_{j=1}^{np} \frac{\lambda_j}{2\pi}\left(\frac{C_v}{2} \ln\left(\frac{Sp_j^2 + 2ASp_j + B}{B} \right) + \frac{D_v - AC_v}{E}\left(\tan^{-1}\frac{Sp_j + A}{E} - \tan^{-1}\frac{A}{E} \right) \right) + \frac{1}{2\pi}\sum_{j=1}^{N_v} \Gamma_k \frac{(x - x_j)}{(x - x_j)^2 + (y - y_j)^2} \tag{8}$$

where $A = -(x - Xp_j)\cos\varphi_j - (y - Yp_j)\sin\varphi_j$, $B = (x - Xp_j)^2 + (y - Yp_j)^2$, $C_u = -\cos(\varphi_j)$, $D_u = x - Xp_j$, $Sp_j = \sqrt{(Xp_{j+1} - Xp_j)^2 + (Yp_{j+1} - Yp_j)^2}$, $E = \sqrt{B - A^2} = (x - Xp_j)\sin\varphi_j - (y - Yp_j)\cos\varphi_j$, $C_v = -\sin(\varphi_j)$, and $D_v = y - Yp_j$.

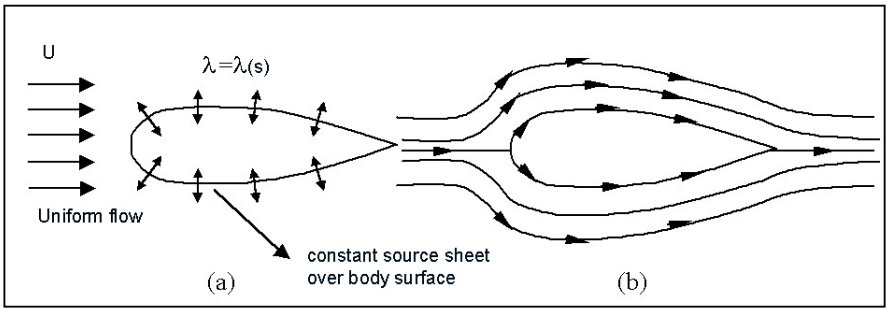

Figure 2. Uniform flow U and constant source strength distribution (λ) combined to construct a flow field around a arbitrary shaped body.

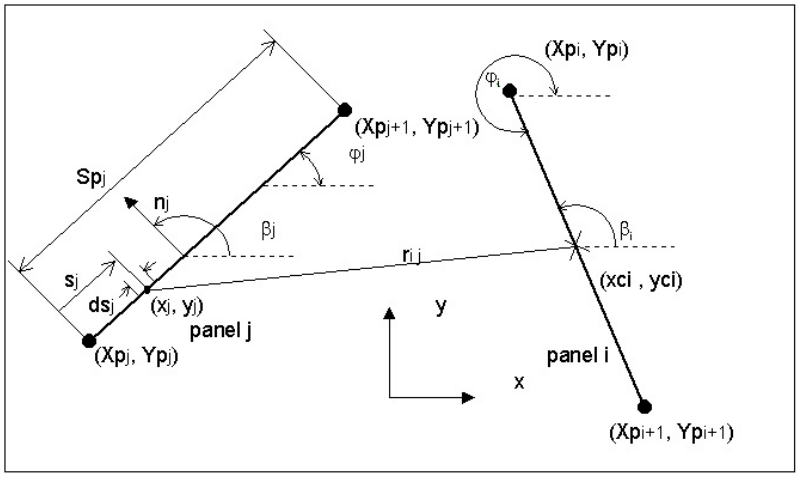

Figure 3.Geometry of panels.

The aerodynamic forces are calculated using the integration of the pressure distribution around the square cylinder, which takes the form of.

$$C_D = \int_{s=0}^{4a} C_p \sin\varphi(s)\, ds \tag{9}$$

and

$$C_L = \int_{s=0}^{4a} C_p \cos\varphi(s) ds \tag{10}$$

where C_D and C_L are the drag and lift coefficients. The pressure field in a point m is calculated as

$$C_P = 1 + 2\left(\sum_{n=1}^{m} \left(\frac{\Gamma_n}{\Delta t} - \Delta u_n \overline{u_n} \right) - \sum_{n=1}^{n_{max}} \left(\frac{\Gamma_n}{\Delta t} - \Delta u_n \overline{u_n} \right) \right) \tag{11}$$

according to Fusen He e Tsung-Chow Su(1998), where

$$\Delta u_n = \left(u_{(+)} - u_{(-)} \right) \tag{12}$$

and

$$\overline{u_n} = \left(\frac{u_{(+)} + u_{(-)}}{2} \right). \tag{13}$$

The velocities $u_{(+)}$ and $u_{(-)}$ are shown in Figure 4.

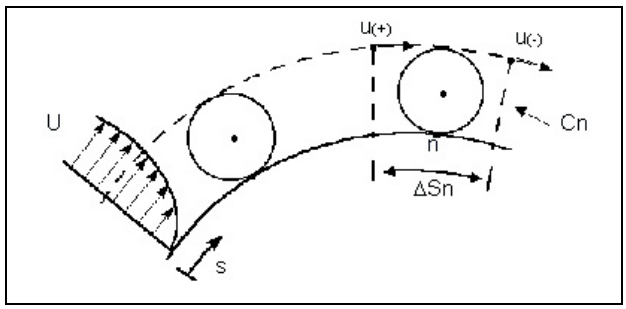

Figure 4. Tangential velocities around point vortex.

3. The Vortex Method

3.1.The Algorithm

The two-dimensional, incompressible, unsteady flow around a circular cylinder formulated above is simulated using a Discrete Vortex Method associated to a Source Panel Method. The Discrete Vortex Method uses an algorithm that splits the convective-diffusive operator (Chorin, 1973) in the form

$$\frac{D\omega}{Dt} \equiv \frac{\partial \omega}{\partial t} + \mathbf{u} \cdot \nabla \omega = 0 \tag{14}$$

$$\frac{\partial \omega}{\partial t} = \frac{1}{Re} \nabla^2 \omega \ . \tag{15}$$

In a real flow vorticity is generated on the body surface so as to satisfy the no-slip condition, Eq. (4), and is transported by convection and diffusion into the flow according to Eq. (6). Our discrete vortex method represents the vorticity by discrete vortices, whose transport by convection and diffusion is carried out in a sequence within the same time step. First, a lagrangian approach is used to simulate the convective process, governed by Eq. (14). The convective motion of each vortex is determined by integration of each vortex path equation, which can be written, using a second-order Adams-Bashforth scheme, as

$$\Delta x_c = \left[\frac{3}{2} u(t) - \frac{1}{2} u(t - \Delta t) \right] \Delta t \tag{16}$$

and

$$\Delta y_c = \left[\frac{3}{2}v(t) - \frac{1}{2}v(t-\Delta t)\right]\Delta t \tag{17}$$

In Eqs. (16) and (17), Δx_c and Δy_c are displacements of a vortex owing to convection, and u and v are components of the velocity at the point occupied by the vortex. Second, the process of viscous diffusion, governed by Eq. (16), is simulated using the Random Walk Method (Lewis, 1991), where the random displacements of each vortex in the x and y directions owing to diffusion, Δx_d and Δy_d, are calculated from

$$\Delta x_d = \Delta r \cos(\Delta\theta) \quad \text{and} \quad \Delta y_d = \Delta r \sin(\Delta\theta), \tag{18}$$

where

$$\Delta r = \left[8Re^{-1}\Delta t \ln(1/P)\right]^{1/2}, \text{ and } \Delta\theta = 2\pi Q \ . \tag{19}$$

In Eqs. (19), P and Q are random numbers between 0 and 1.

In order to remove the singularity of the point vortices we use Lamb vortices for $r \le \sigma_o$, where σ_o is the radius of the vortex core. During a time step Δt, the core grows from zero to σ_o, where

$$\sigma_o = 4.48364\sqrt{\frac{\Delta t}{Re}}\ . \tag{20}$$

This value is kept constant for the entire simulation. In terms of σ_o, the dimensionless velocity induced by the k^{th}-vortex in the circumferential direction, u_{θ_k}, is

$$u_{\theta k} = \Gamma_k / 2\pi r \{1 - \exp[-C(r^2/\sigma_o^2)]\}\ . \tag{21}$$

In this particular equation r is the radial distance between the vortex center and the point in the flow field where the induced velocity is calculated, and $C = 5.02572$ is a constant. The distance ε off the cylinder surface where the new vortices are generated per time step (Fig. 5) is set equal to σ_o for all the cases studied.

The time step Δt is calculated from an estimate of the convective length and velocity scales of the flow. For a length scale Δs between vortices generated at the surface (~4a/N) and a velocity scale of order one, we can write

$$\Delta t = \frac{4k}{N}\ . \tag{22}$$

In Eq. (22), $0 < k \le 1$, and N is the number of vortices generated per time step.

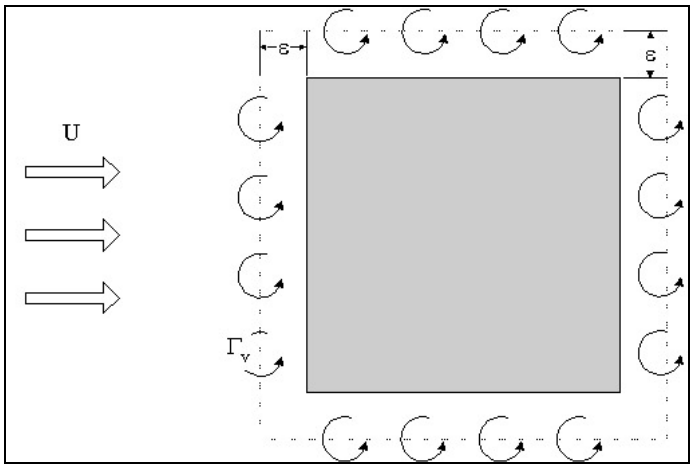

Figure 5. Vortex generation scheme.

4. The Numerical Implementation

The numerical method described above is implemented essentially in five steps: (i) generation of new vortices; (ii) calculation of the forces on the body; (iii) convection of the vortices; (iv) diffusion of the vortices; (v) elimination of some vortices; (vi) stepping in time.

The process of vorticity generation is carried out so as to satisfy the condition impermeability and the no-slip condition, Eqs. (3) and (4). At each time step, N new vortices are created a small distance ε off the body surface with a uniform distribution, and new N source strength are created over the panels that covers the body. The strengths of these new vortices and the source panels strengths are determined by imposing the no-slip condition and the impermeability condition at N−1 control points on the cylinder surface, at the center of each panel.(Fig. 3). In order to implement the entire procedure, the velocities induced by all the vortices in the wake (and their images) are computed at the N−1 points where Eqs. (3) and (4) must be satisfied. This contribution is added to the velocities induced by the new vortices and the source strengths and equated to zero. Thus, 2N−2 equations can be written out for the 2N unknowns (N new vortices and new N source strenghs). The two last equations are statements of conservation of circulation (the sum of all vortices with known and unknown strengths must equal zero) and mass conservation (the sum of all new source strengths must equal zero). This procedure yields an algebraic system of N equations and N unknowns, that is,

$$u_n = \sum_{k=1}^{N} \left(A_{jk}\Gamma_k(t) + B_{jk}\lambda_k \right) = b_j(t), \qquad 1 \le j \le N-1. \tag{23}$$

$$u_t = \sum_{k=1}^{N} \left(C_{jk}\Gamma_k(t) + D_{jk}\lambda_k \right) = b_j(t), \qquad 1 \le j \le N-1. \tag{24}$$

$$\sum_{k=1}^{N} \lambda_k(t) = b_N(t), \qquad j = N. \tag{25}$$

$$\sum_{k=1}^{N} \Gamma_k(t) = b_N(t), \qquad j = N. \tag{26}$$

The 2N×2N matriz given by Eqs (23) to (26) takes the form of

$$A = \begin{bmatrix} A_{jk} & B_{jk} \\ 1 & 0 \\ C_{jk} & D_{jk} \\ 0 & 1 \end{bmatrix} \tag{27}$$

The N× N matrix A_{jk} represents the coefficient matrix of the normal velocities induced by the vortices, the N× N matrix B_{jk} represents the coefficient matrix of the normal velocities induced by the source panels, the N× N matrix C_{jk} represents the coefficient matrix of the tangential velocities induced by the vortices, and the N× N matrix D_{jk} represents the coefficient matrix of the tangential velocities induced by the source panels. The second and fourth rows represent the conservation of vorticity and the conservation of mass in the last panel (it means the no-slip and the impermeability conditions are not satisfied in the control point of the last panel).

The linear system is given by

$$\begin{bmatrix} A_{jk} & B_{jk} \\ 1 & 0 \\ C_{jk} & D_{jk} \\ 0 & 1 \end{bmatrix} \cdot \begin{bmatrix} \Gamma_k \\ \lambda_k \end{bmatrix} = \begin{bmatrix} bj \\ \end{bmatrix}. \tag{28}$$

The elements of the 2N×2N matrix, A, depend on the position of the vortices just created and on the points on the cylinder surface where the no-slip and impermeability conditions (control points of panels) are imposed. It is, therefore, calculated only once for the entire simulation. The vector b_j, which is recalculated every time step, includes the contribution of all the terms in Eq. (7). The vortices that penetrate the body are reflected.

5. Results and Analysis

We now present the results for the simulation of the high Reynolds number, two-dimensional, incompressible, unsteady flow around a square cylinder. Long-time simulations were performed with 200 vortices generated per time step and t = 40.00. Here, only the case Re = 10^5 was chosen. Furthermore, the experimental drag coefficient and Strouhal number for Re = 10^5 are in a range where they are approximately constant with respect to the Reynolds number. The numerical parameters used in the computations are: $\Delta t = 0.1$ and $\varepsilon = \sigma_o = 0.0045$. This run ended with 80000 vortices.

Table 1. Comparison of the mean drag coefficient and Strouhal number with other numerical and experimental results, for Re = 10^5.

Re = 10^5	C_D	St
Blevins (1985): experimental	2.20	0.120
Vickery (1966)	2.05	0.118
Present simulation	1.88	0.138

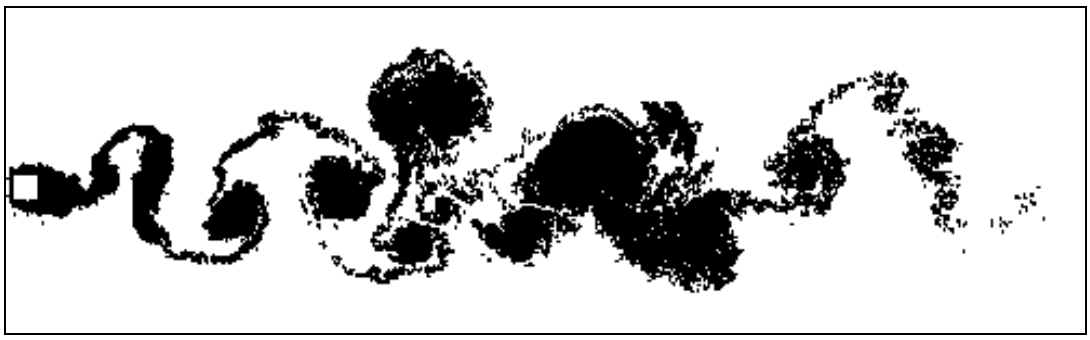

Figure 6. Positions of the wake vortices for Re = 10^5, at t = 40.00; N = 200, $\Delta t = 0.1$ and $\varepsilon = \sigma_o = 0.0045$.

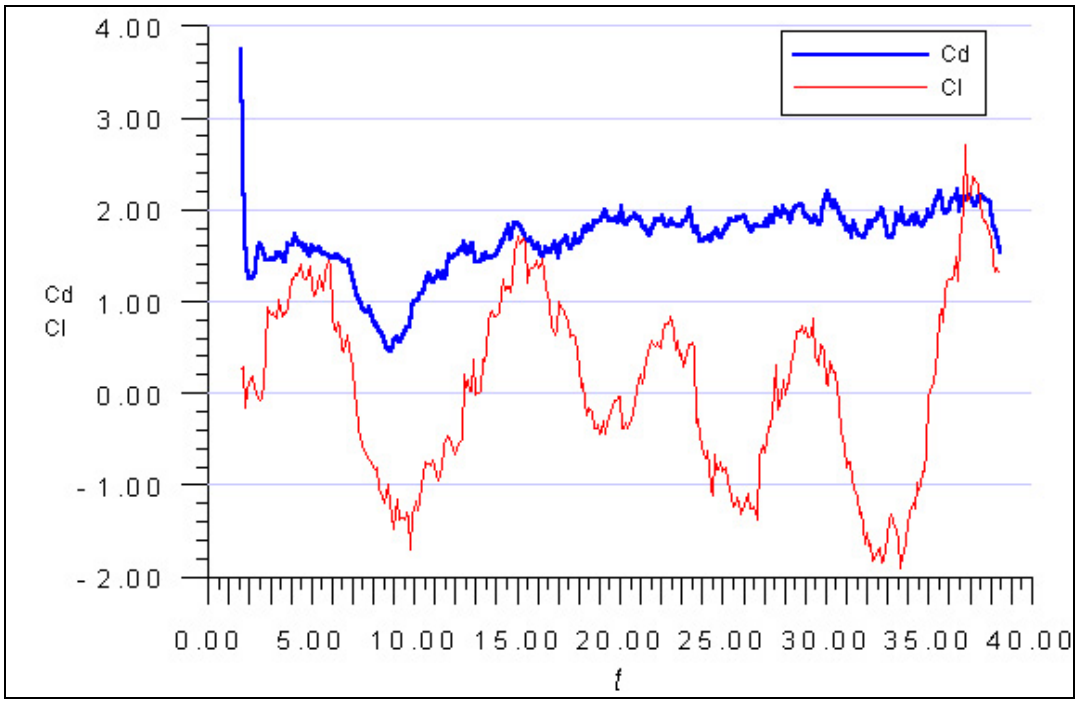

Figure 7. Time variation of C_D and C_L for Re = 10^5, at t = 40.00; N = 200, $\Delta t = 0.1$ and $\varepsilon = \sigma_o = 0.0045$.

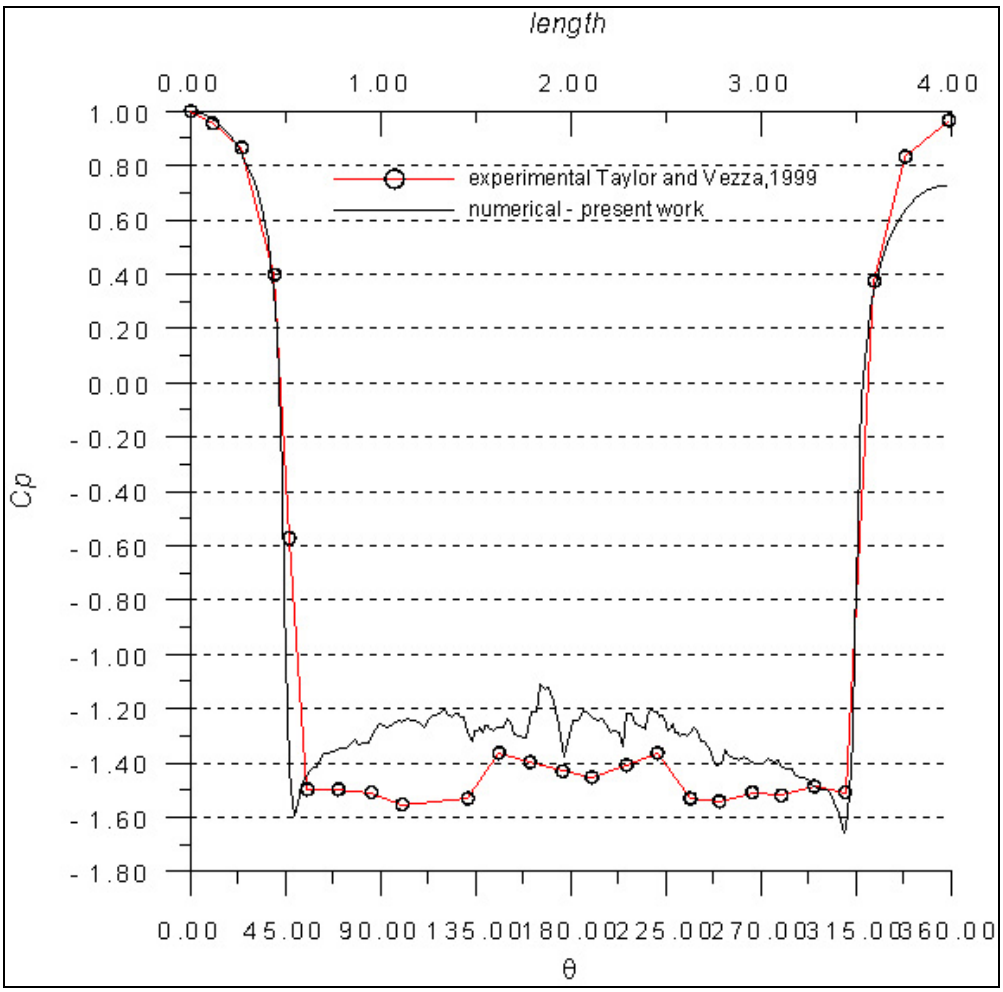

Figure 8. Cp average at t = 40.00 for Re = 10^5, N = 200, $\Delta t = 0.1$ and $\varepsilon = \sigma_o = 0.0045$.

The flow around a circular cylinder presents several interesting characteristics, which can be described starting with the occurrence of the separation phenomenon. Experiments show the formation of the so-called Von Karman vortex street, which is comprised of large vortices generated and shed alternately from the upper and lower surfaces of the cylinder. The vortices in the wake are connected in pairs by a vortex sheet. Owing to the periodic characteristics of the wake, the lift force on the cylinder oscillates in time around zero, with a frequency determined by the Strouhal number. The periodic behavior of the wake is also reflected on the drag force, which presents a time evolution that oscillates around a non-zero mean value. However, its non-dimensional frequency is twice the Strouhal number, since the drag force reaches its maximum value twice for each cycle of the lift force. For these reasons, the experimental values available in the literature represent time averages for the lift and drag coefficients.

Fig. 6 illustrates the positions of the vortices present in the flow simulation at t = 40.00. The wake clearly shows the occurrence of separation on the corners of the square cylinder surface, followed by the generation and growth of the separated vortices on the back of the cylinder, which precedes their shedding into the wake. It can also be seen the formation of pairs of the large eddies that comprise the Von Karman vortex street, connected to each other by thin vortex sheets. The cores of these large vortices grow as they move downstream of the cylinder due to the diffusive effect of the flow. Note that the farthest vortices in the wake were generated at the initial moments of the simulation, and they are, therefore, subject to a numerical transient effect.

The time histories of the lift and drag coefficients are revealed in Fig. 7. As expected these coefficients reach a periodic steady state after an initial numerical transient (about 20 units of non-dimensional time), where they oscillate in time with approximately constant amplitude. The lift coefficient oscillates about zero with a non-dimensional frequency (Strouhal number, St) of 0.138. This value, calculated using the C_L peaks at t = 22.5 and t = 37.0, is a little higher than the experimental one of Blevins' (1984), who measured 0.12. On the other hand, the drag force oscillates about a mean value of 1.88 (integrated over the same cycle used to determine St), with a non-dimensional frequency approximately equal to twice the Strouhal number. The experimental mean drag coefficient of Blevins' is 2.20, whereas the numerical value of Vickery (1966) is 2.05. The comparison of our simulation with the experimental results of Blevins (1984) and the numerical results of Vickery (1966) are shown in Table 1 for easy comparison.

A new implementation for the calculation of the coefficient of pressure, based in the work of Fusen He e Tsung-Chow Su(1998), was tested with better results (see Fig.8) in comparison with the scheme presented by Lewis (1991).

5. Conclusions

The results presented in this paper are close to the experimental ones, but it can be improved in order to get more accurated values concerning the Strouhal number and the drag coefficient, which both relative errors were about 15%. In this paper, a new implementation for the calculation of the pressure coefficient was tested with good results. New simulations will be carried out with more vortices generated per time step and a scheme of Multipole Expansion to reduce the computation times.

5. References

Blevins, R.D., 1984, " Applied Fluid Dynamics Handbook", Van Nostrand Reinhold Co.

Chorin, A.J., 1973, "Numerical Study of Slightly Viscous Flow", *Journal of Fluid Mechanics,* Vol. 57, pp. 785-796.

Fusen HE e Tsung-Chow Su, 1998, "A Numerical study of bluff body aerodynamics in high Reynolds number flows by viscous Vortex Element Method", Journal of Wind Engineering and Industrial Aerodynamics, Vols.77 e 78, pp.:.393-407.

Lewis, R.I., 1991, "Vortex Element Methods for Fluid Dynamic Analysis of Engineering Systems", Cambridge University Press, Cambridge.

Taylor, I. And Vezza,M., 1999, "Prediction of unsteady flow around square and rectangular section cylinders using discrete vortex method", Journal of Wind Engineering and Industrial Aerodynamics, Vol. 82, pp.: 247-269.

Vickery, B.J., 1966, "Fluctuating lift and drag on a long cylinder of square cross-section in a smooth and in a turbulent stream", Journal Fluid Mechanics, Vol. 25, pp.:481-494.